

Hand Orientation Estimation in Probability Density Form

Kazuaki Kondo
Kyoto University
Kyoto, Japan

kondo@media.kyoto-u.ac.jp

Daisuke Deguchi
Nagoya University
Aichi, Japan

ddeguchi@nagoya-u.jp

Atsushi Shimada
Kyushu University
Fukuoka, Japan

atsushi@ait.kyushu-u.ac.jp

Abstract

Hand orientation is an essential feature required to understand hand behaviors and subsequently support human activities. In this paper, we present a new method for estimating hand orientation in probability density form. It can solve the cyclicity problem in direct angular representation and enables the integration of multiple predictions based on different features. We validated the performance of the proposed method and an integration example using our dataset, which captured cooperative group work.

1. Introduction

Recognizing hands in videos is one of fundamental approaches to understanding human-to-human and human-to-environment interaction. Previous studies have approached detecting hands in various scenes, including daily snapshots[1], driving vehicles[9] and interaction captured from ego-centric cameras[6]. Currently, the performance of hand detection has almost reached the level of practical use. For the next step, in this study, we propose an approach to estimate hand orientation in an image as an important attribute for deeper analysis. Hand orientation can provide a better understanding of hand poses or interaction direction.

A major issue when estimating the orientation of an object in an image is the cyclicity in angular representation. In particular, 0 and 2π radians are quite distant in terms of angular representation, but they correspond to the same orientation. An orientation estimation method that does not consider this cyclicity results in inaccurate angles. The experiments presented by Deng et al. [2] illustrated that direct angle representation leads to poor performance in hand orientation estimation. Qu et al. [5] assumed that regression errors are large at a singular angle, but do not propagate to the angles far from it. They used a three-path-way convolutional neural network (CNN) that independently estimates

three angular values that correspond to the same orientation in the image, but have different origin angles. The final output is determined by majority voting of the three estimated angles because one of them may have a great influence on the cyclicity, whereas the remaining two do not. Instead of angular representation, Schuch et al. [4] and Yang et al. [10] proposed representing orientation using a vector whose components are projections onto the horizontal and vertical axes. These component values are continuous at an arbitrary angle and their combination has a one-to-one correspondence to the orientation. Thus, cyclicity does not have to be considered.

In the present study, we propose another representation: probability density form $p(\theta)$, which is different from direct angle θ or vector $(\cos\theta, \sin\theta)$ mentioned above. This representation has the following two advantages:

- Estimating $p(\theta)$ instead of θ can avert the cyclicity problem. The change of estimation target (dimension) is a similar approach to vector representation.
- In most cases in previous works, only a rectangular hand region was used for estimating hand orientation. However, we often have other valuable features, such as the hand position in the image or relative geometry to other body parts. When multiple estimation results that use individual features are all represented in probability density form, they can be integrated easily.

In this paper, we explain an approach to apply the probability density form to a CNN framework and an example of integrating multiple estimation results. We evaluate the performance of the proposed method on an original dataset that captures cooperative group work.

2. Methodology

2.1. Orientation estimation in density form

In recent years, CNN-based methods have achieved promising results in generic image recognition. Thus, we apply our density form approach to a typical image-based

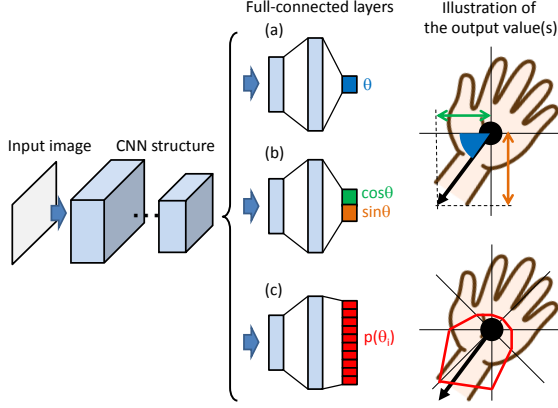


Figure 1. Comparison of CNN structures for hand orientation estimation: (a) direct angular representation; (b) vector presentation; and (c) our probability density form and its illustration in radar chart style.

CNN that accepts a rectangular image as its input. The proposed method describes the probability density of hand orientation in a non-parametric and discrete form, $p(\theta_i)$, where $\theta_i = \frac{2\pi i}{N}$, $i = 0, 1, 2, \dots, N-1$. For this representation, an N -path CNN estimates N probability values $p(\theta_i)$ at its output layer instead of one angular value for the direct representation or two projected values for the vector representation (Fig. 1). The softmax activation function is applied at the output layer to meet the probability density condition $\sum_i p(\theta_i) = 1$. These are the only requirements of the proposed method; we do not have any other constraints on the CNN structure, including its former layers. Our probability density form can be applied to any type of CNN.

Alternatively, we need to convert ground truth orientations into density forms to use them for training the CNN, and recover the orientation angle from the estimated probability density. This mutual conversion is used as follows:

Orientation angle to probability density

Assume not only ground truth orientation θ_{gt} but also its neighborhood orientation $\theta_{neighbor}$ has a likelihood in $p(\theta_{gt}) > p(\theta_{neighbor}) > 0$ relations; that is, orientations close to the ground truth are acceptable as estimated values. Using this assumption, probability density $p(\theta_i)$ is determined as

$$p(\theta_i) = \frac{1}{s_{vd}} \exp\left(-\frac{d(\theta_i, \theta_{gt})^2}{2\sigma^2}\right) \quad (1)$$

$$d(\theta_1, \theta_2) = \text{acos}((\cos\theta_1, \sin\theta_1) \cdot (\cos\theta_2, \sin\theta_2))$$

from ground truth orientation θ_{gt} , where σ denotes the acceptable degree described by the Gaussian distribution. s_{vd} is a normalization term for $\sum_i p(\theta_i) = 1$. Through the vector inner product form, angular distance $d(\theta_1, \theta_2)$ averts the cyclicity problem.

Probability density to orientation angle

Optimal orientation angle θ is estimated using an inverse

approach to the above process:

$$\theta = \text{argmax}_\theta \frac{\sum_i p(\theta_i) \exp\left(-\frac{d(\theta_i, \theta)}{2\sigma^2}\right)}{\sum_i p(\theta_i)} \quad (2)$$

based on cosine similarity between $\{p(\theta_i)\}$ and $\mathcal{N}(\theta, \sigma)$.

2.2. Integration of multiple densities

The visual pattern of a hand region strongly reflects hand orientation; however, other features are often useful as well. The integration of estimation results using multiple features improves performance. As an example, we present two additional estimation methods for hand orientation and integrate them into $p(\theta_i|H_{img})$, which is estimated by the proposed method that uses only hand region image H_{img} .

Human region-based estimation: $p(\theta_i|H_r)$

Because the hand is the endpoint of the human body, human region H_r definitely appears in the neighborhood of the hand in the image. This feature provides a somewhat weak but valuable additional constraint for hand orientation. Probability density $p(\theta_i|H_r)$ is given by the amount of the human region that lies in each orientation θ_i :

$$p(\theta_i|H_r) = \frac{1}{s_h} \sum_{r=R}^{K_R R} H_r(cx + r\cos\theta_i, cy + r\sin\theta_i)$$

$$H_r(x, y) = \begin{cases} 1 & (x, y) \text{ is in the human region} \\ 0 & \text{otherwise} \end{cases} \quad (3)$$

where (cx, cy) , R and s_h denote the center coordinate of the hand region, half the size of the hand and a normalization term for $\sum_i p(\theta_i|H_r) = 1$, respectively. K_R determines the upper limit of the neighborhood region of the hand.

Position-based estimation: $p(\theta_i|cx, cy)$

The appearance and position of the hand in the image often depends on the target scenario or camera location, which is used to provide some constraint on hand orientation. The tracking and recognition of a hand presented by Lee et al. [7] used a hand position constraint in first-person videos that captured interactions in a face-to-face style. Using a similar idea, the position of the hand provides a constraint on hand orientation. To predict the hand orientation probability at an arbitrary position in the image, we use an interpolation of the probability densities at grid points (gu_k, gv_k) in the neighborhood of target position (cx, cy) :

$$p(\theta_i|cx, cy) = \frac{\sum_k w_b(gu_k, gv_k, cx, cy) p(\theta_i|gu_k, gv_k)}{\sum_k w_b(gu_k, gv_k, cx, cy)} \quad (4)$$

where $w_b(gu, gv, cx, cy)$ denotes a bilinear weight that represents the contribution amount of grid point (gu, gv) to target position (cx, cy) . The probability densities at grid points $p(\theta_i|gu_k, gv_k)$ are trained as weighted means of M ground truth samples $p(\theta_i|x_j, y_j)$, $j = 1, 2, \dots, M$.

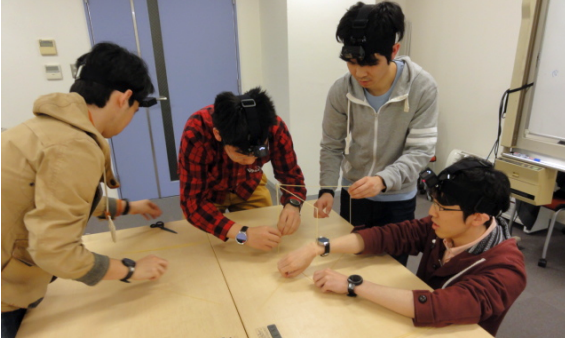


Figure 2. Example scene of the group work task.

When we assume that the visual pattern of the hand region, human region in the neighborhood of the hand and hand position on the image are independent features, their integrated estimation is given by the simple product of the individual probability densities. The optimal orientation angle that matches the integrated probability density $p(\theta_i | H_{img}, H_r, cx, cy)$ can be extracted using the same approach explained in Eq. (2).

3. Experimental evaluation

3.1. Dataset

Our motivation for estimating hand orientation is to use it to analyze interactions in cooperative group work. In the experimental evaluation, we used first-person view videos captured from head-mounted cameras on the group work participants. A cooperative assembly task was given to the participants, which was building a tower using dried pastas, adhesive tape and thread, with a marshmallow on the top, known as the ‘‘Marshmallow Challenge’’ (Fig. 2). It is often used for ice breaking or community building, but it can be used as a good example to observe cooperative interaction because the participants must build a tower as high as they can with quite limited/weak materials, within short time. We conducted the group work task for two groups that consisted of four university students. We captured a total of 17 min. \times 8 first-person videos in 1920×1080 pixels. We manually extracted over 10 thousand hands from the videos with their bounding boxes and orientations running from the palm centers to the wrist centers. We used this dataset as the ground truth for training and verifying the estimated results.

3.2. Experimental configuration

Density form estimation can be applied easily to any type of CNN structure. For the early stage validation, we selected a simple CNN that combined the convolutional part of VGG16[8] and a 1,024-dimension fully connected layer. The hand region images were resized to 112×112 pixels to be inserted into the CNN. The sampling resolution of the orientation and the Gaussian variance for value-density mu-

tual conversion were configured as $N = 16$ and $\sigma = 10^\circ$, respectively. KL divergence was used as the loss function to maximize the distribution similarity during parameter training. Training started from the pre-trained parameters using the imageNet dataset. The last layer of the VGG16 convolutional part and the additional fully connected layers were fine-tuned using our dataset. To prevent overfitting, we also used the dataset augmentation trick, which applied a combination of random shift and expansion to the original hand images. In the additional estimation methods, human regions were extracted by the pre-trained PSPNet[3]. The neighborhood regions were defined using $K_R = 4.0$, considering the ratio of the hand size and wrist-to-elbow distance. The grid size for position-based estimation was 5×4 along the image’s horizontal and vertical axes.

The comparative methods were a simply estimating one angle as a baseline, the angle duplication and the vector representation. The last two methods were configured in reference to [5] and [10], respectively. The mean squared error was used as the loss function in those methods. The other conditions were all the same as those used in the proposed method. Performance validation was conducted using 10-fold cross validation.

3.3. Results and discussion

Figure 3 illustrates the estimated results on the group work FPV dataset when applying probability density representation $p(\theta_i | H_{img})$ to orientation estimation that uses only the hand region images. We can see that the radar chart visualization of the probability density is strongly biased to the wrist direction, and the final orientation results indicated by the green lines are close to the ground truth indicated by the red lines.

For statistical analysis, we calculated the percentages of samples whose estimation errors were within particular angles. The performance comparison in Table 1 and Fig. 4 shows those percentage values among the validated three methods. Even the proposed method using only hand region images achieved a significant improvement in the ‘‘less than $10^\circ, 20^\circ, 30^\circ$ ’’ categories compared with the conventional methods. We have two hypothetic reasons for the accuracy improvement.

1. The conventional methods try to find correct orientation, but not to omit incorrect orientation. In contrast, the probability density approach achieves both of them, because CNN training proceeds to increase probability values at θ_i close to the ground truth and to suppress probability values at other orientations, simultaneously.
2. Orientation is not a label, but a scalar. Additionally, nobody can know (or define) precise hand orientation values under various hand pose including finger form

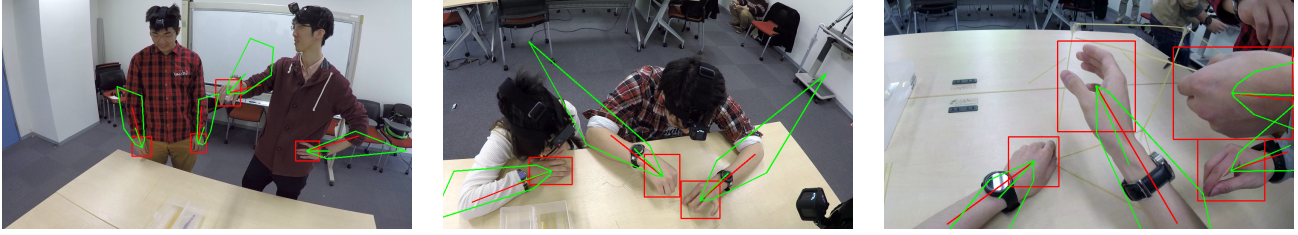


Figure 3. Examples of the estimation results. The red lines running from the hand centers denote the ground truth hand orientations. The green charts and lines correspond to estimated probability density $p(\theta_i|H_{img})$ and the final orientation prediction, respectively.

Table 1. Orientation error populations

Method	$< 10^\circ$	$< 20^\circ$	$< 30^\circ$	\dots	$> 90^\circ$	$> 120^\circ$	$> 150^\circ$
baseline	35.3%	61.9%	77.5%	-	3.22%	1.73%	0.834%
duplicated angles[5]	40.9%	69.7%	85.2%	-	0.702%	0.197%	0.056%
vector representation[10]	41.3%	70.0%	85.8%	-	0.448%	0.224%	0.126%
density representation	61.5%	88.0%	95.1%	-	0.731%	0.431%	0.234%
integrating multiple density	65.2%	90.0%	96.1%	-	0.553%	0.403%	0.197%

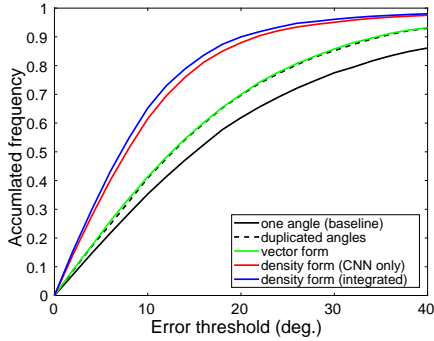


Figure 4. Visual comparison of the orientation error populations.

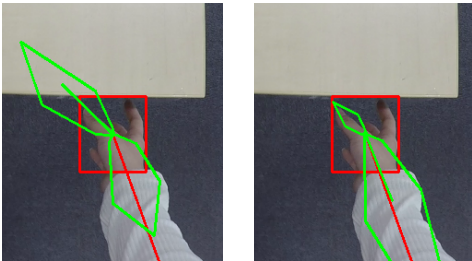


Figure 5. Improvement by integration. (left) large orientation error given by $p(\theta_i|H_{img})$. (right) correct orientation given by $p(\theta_i|H_{img}, H_r, cx, cy) = p(\theta_i|H_{img})p(\theta_i|H_r)p(\theta_i|cx, cy)$.

and connection to wrist joint. Ground truth values have certain ambiguity due to those reasons. The probability distribution given by Eq. (1) successfully handles this issue. Note that correct σ should be configured to get this effect.

However, the proposed method slightly increased the frequencies in the “more than 90° , 120° , 150° ” categories. This disadvantage was also caused by the use of the proba-

bility density form. Essentially, the N -path CNN individually predicted N values, even if the softmax normalization at its last layer provided some dependency among them. This characteristic may deliver multiple peaks at distant orientations in $p(\theta_i)$, despite being inconsistent with the actual scenario. As an example of an extreme case for intuitive understanding, assume two similar hand images with quite different ground truth orientations are provided for training. In the probability density scheme, the CNN parameters are optimized to output two distinct peaks at the two ground truth orientations. When an incorrect peak is selected as a final prediction, its error becomes large. By contrast, the CNN that uses the vector representation is trained to output the mean of the two ground truth orientations, which can avoid large orientation errors. This analysis is supported by the typical failure example shown on the left of Fig. 5. The estimated probability density has two peaks at distant orientations in the estimated probability density: one is close to the ground truth, but the other is quite far from it.

The above disadvantage can be reduced by integrating multiple estimations, as shown on the right of Fig. 5. Particularly, the human region-based method constrains the possible range of hand orientation, which suppresses incorrect selection from multiple peaks in $p(\theta_i|H_{img})$. The integration also provides a further improvement in the “less than 10° , 20° , 30° ” categories, as shown in Table 1. The proposed scheme provides a choice of integration for further accuracy. However, the additional two methods also have issues. The human region does not work well when the hand lies in the body region. Additionally, we confirmed that the hand orientation prior based on its position strongly depends on the scene, such as discussion using a white board and cooperative assembly work. The simple product of the probability densities assumes that all the integration targets

have the same confidence and does not consider the weights among them.

4. Conclusion

In this paper, we proposed predicting hand orientation in probability density form. On the group work FPV dataset, the proposed method estimated hand orientation more accurately than the conventional vector representation method. Additionally, we easily integrated multiple results represented in the probability density form and confirmed that it leads to improved performance. For further accuracy, the probability density form should be applied to an advanced CNN structure with a fusion of multiple scale features. The additional estimation methods, including their integration scheme, must be improved.

References

- [1] A. Zisserman A. Mittal and P. H. S. Torr. Hand detection using multiple proposals. In *In Proc. of the British Machine Vision Conference*, 2011. 1
- [2] X. Deng, Y. Zhang, S. Yang, P. Tan, L. Chang, Y. Yuan, and H. Wang. Joint hand detection and rotation estimation using cnn. *IEEE transactions on Image Processing*, 27(4):1888–1900, 2017. 1
- [3] X. Qi X. Wang H. Zhao, J. Shi and J. Jia. Pyramid scene parsing network. In *In Proc. of the IEEE Conf. on Computer Vision and Pattern Recognition*, pages 2881–2890, 2017. 3
- [4] S. Schulz P. Schuch and C. Busch. Convnet regression for fingerprint orientations. In *In Proc. of Scandinavian Conference on Image Analysis*, pages 325–336, 2017. 1
- [5] Z. Qu, J. Liu, Y. Liu, Q. Guan, C. Yang, and Y. Zhang. Orient: A regression system for latent fingerprint orientation field extraction. In *In Proc. of Artificial Neural Networks and Machine Learning*, pages 436–446, 2018. 1, 3, 4
- [6] D. Crandall S. Bambach, S. Lee and C. Yu. Lending a hand: Detecting hands and recognizing activities in complex egocentric interactions. In *In Proc. of the IEEE Int. Conf. on Computer Vision*, pages 1949–1957, 2015. 1
- [7] J. M. Franchak S. Lee, S. Bambach. D. J. Crandall and C. Yu. This hand is my hand: A probabilistic approach to hand disambiguation in egocentric video. In *In Proc. of IEEE Int. Conf. on Computer Vision and Pattern Recognition*, 2014. 2
- [8] K. Simonyan and A. Zisserman. Very deep convolutional networks for large-scale image recognition. In *Large Scale Visual Recognition Challenge*, 2014. 3
- [9] C. Zhu C. N. Duong K. Luu T. H. N. Le, K. G. Quach and M. Savvides. Robust hand detection and classification in vehicles and in the wild. In *In Proc. of IEEE Int. Conf. on Computer Vision and Pattern Recognition*, pages 1203–1210, 2017. 1
- [10] L. Yang, Z. Qhi, Z. Liu, S. Zhou, Y. Zhang, H. Liu, J. Wu, and L. Shi. A light cnn based method for hand detection and orientation estimation. In *In Proc. of Int. Conf. on Pattern Recognition*, pages 2050–2055, 2018. 1, 3, 4